p-Version Mesh Generation Issues

Xiao-Juan Luo, Mark S. Shephard, Jean-François Remacle
Scientific Computation Research Center, Rensselaer Polytechnic Institute, Troy, NY 12810,
xluo@scorec.rpi.edu, shephard@scorec.rpi.edu, remacle@scorec.rpi.edu
Robert M. O'Bara, Mark W. Beall
Simmetrix, Inc., Troy, NY 12180
obara@simmetrix.com, mbeall@simmetrix.com
Barna Szabó
Washington University, St. Louis, MO 63130
szabo@me.wustl.edu
Ricardo Actis
Engineering Software Research and Development, Inc., St. Louis, Missouri
ricardo@esrd.com

ABSTRACT

Higher order (p-version) finite element methods have been shown to be clearly superior to low order finite element methods when properly applied. However, realization of the full benefits of p-version finite elements for general 3-D geometries requires the careful construction and control of the mesh. A 2-D elasticity problem with curved boundary is used to clearly illustrate the influence of the mesh shape geometric approximation order and shape representation method on the accuracy of finite element solution in a p-version analysis. Consideration is then given to a new approach for the representation of mesh geometry for p-version meshes and to the automatic generation of p-version meshes.

Keywords: geometric approximation, Bezier polynomials, curvilinear mesh

1. INTRODUCTION

High order (p-version) finite element methods, characterized by the capability of exponential rate of convergence, are gaining popularity in industry. The basic functions of p-version finite elements, their convergence properties and aspects of their computer implementation have received extensive consideration in the literature (e.g. [1,3,10,16,17,18]). However, the critical technical issues of the appropriate geometric representation of p-version finite elements for solving partial differential equations over general three dimensional domains have not received adequate consideration. This paper first demonstrates that the accuracy of finite element solutions is strongly influenced by how well the geometry is approximated. Consideration is then given to a set of procedures being developed for proper generation of curved elements for p-version analyses.

Section 2 outlines the advantages of p-version finite elements assuming the proper choice of meshing and mapping procedures as required to preserve the superior rates of convergence. Section 3 examines the role of the mesh geometric approximation on the accuracy of the results obtained in terms of a specific curved domain problem with a known exact solution. This simple example clearly demonstrates that the use of quadratic geometric approximations for p-version finite elements does not lead to satisfactory solution results, in the sense that using p-levels greater than 3 or 4 will produce results that are affected by the errors in mapping.

The requirements of Section 2 and results of Section 3 demonstrate the need for new mesh generation technologies to support p-version finite elements. Section 4 overviews current efforts on the development of such a mesh generation capability. Central to this new approach is the use of Bezier basis for the geometric representation of the element shapes. This basis allows one to effectively increase the order of geometric appropriation in an efficient manner to any order desired. In addition, this basis supports effective methods for the execution of key operations such as determining the validity of curved finite elements and determining which mesh entities require shape change to make an invalid element valid.

2. p-VERSION FINITE ELEMENT MESHES

A finite element mesh serves two purposes: First, to allow representation of an arbitrary body by a collection of elements on which piecewise polynomial functions (occasionally augmented by other functions) are defined, and second, to control the error of approximation in terms of the data of interest.

The error of approximation depends on the finite element mesh and the polynomial degree of elements. In conventional FEA codes, the polynomial degree of elements are

fixed at 1 or 2, and the error is controlled by making sufficiently fine meshes: The diameter of the largest element is denoted by h. The errors of approximation are reduced as h is reduced. The term h-version refers to this approach. Since the mid-1980's an alternative, known as the p-version, matured sufficiently for use in professional practice. In this approach the primary role of the mesh is to represent the topological and geometric description of the object being modeled by a collection of elements and the error is controlled by the polynomial degree of elements, denoted by p. The error is reduced as p is increased. The p-version has certain advantages, which include faster rates of convergence and the ability to produce a sequence of solutions, corresponding to increasing p, automatically and without the need to alter the finite element mesh (so long as the mesh provides a satisfactory geometric approximation to the domain). This allows monitoring the convergence of the data of interest and estimating the errors of approximation. A large number of papers are available on this subject, see, for example, references [1,10,11,12,13,14].

The p-version poses certain new requirements for meshing. Since the size of elements is much larger than in the h-version, it is essential to use advanced mapping procedures so that the domain geometry is properly represented and integrated. Various procedures have been developed and implemented using special collocation points, known as the Babuska points, in connection with blending function techniques see, for example, references [2,7]. A typical finite element mesh used in the p-version is shown in Figure 1. The solution, representing the von Mises stress contours, was obtained with StressCheck†.

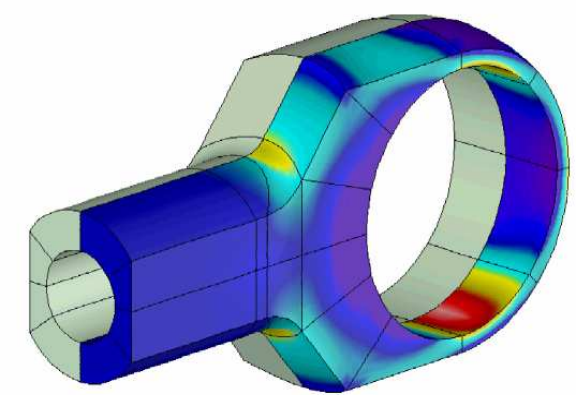

Figure 1. A typical finite element mesh in the p-version.

The proper choice of the mesh topological and geometric representation depends on the goals of computation. In solid mechanics the goals of computation are: (a) to determine stiffness characteristics of a structure, including natural frequencies; (b) to determine the strength characteristics, including stress maxima and stress intensity factors, and (c) to determine stability limits (buckling loads). In stiffness and stability computations it is generally possible to simplify meshing by omitting small features, such as fillets, bosses, small holes, etc. In strength computations, when the goal is to compute the maximal stress, it is necessary to include fillets and all relevant features at least within the region where the maximal stress is sought. This is known as the region of primary interest. A frequent conceptual error in finite element analysis is reporting stresses in regions where the fillets and other small features were omitted.

The error of approximation has two sources: the local error and the pollution error. The pollution error, associated with the region of secondary interest, is controlled by ensuring that the error in the natural norm of the formulation, usually the energy norm, is sufficiently small. The local error, associated with the region of primary interest, depends on the local discretization (choice of mesh, mapping and the polynomial degree). This error is most efficiently controlled by the p-version of the finite element method.

3. INFLUENCE OF GEOMETRIC APPROXIMATION

This section discusses the influence of geometric approximation on the solution accuracy of p-version finite element method by using a benchmark two-dimensional elasticity problem for which analytic expressions for the exact displacement and stress field are known.

3.1 Model problem

An infinite plane weakened by an elliptical hole is deformed by the application of uniform tensile stress in the vertical direction at infinity as shown in Figure 2a. The relevant geometric parameters are the major axis a and minor axis b of the inner ellipse. These parameters are typically related to a third parameter, m, as

$$a = 1 + m,\ b = 1 - m,\ 0 \le m < 1 \qquad (1)$$

where $m = 0$ corresponds to a circle and $m = 1$ is a sharp crack.

Due to the double symmetry of the problem, only one quarter of the sub-domain ABCDE needs to be investigated as shown in Figure 2b. The exact stresses for the infinite domain problem are known along edges BC and DC and given by:

$$\sigma_x = \frac{1}{2}(S(1 - \cos 2\theta) + 2\tau_{\rho\rho}\cos 2\theta - 2\tau_{\rho\theta}\sin 2\theta) \qquad (2)$$

$$\sigma_y = \frac{1}{2}(S(1 + \cos 2\theta) + 2\tau_{\rho\rho}\cos 2\theta + 2\tau_{\rho\theta}\sin 2\theta) \qquad (3)$$

$$\sigma_{xy} = \frac{1}{2}((\tau_{\rho\rho} - \tau_{\theta\theta})\sin 2\theta + 2\tau_{\rho\theta}\cos 2\theta) \qquad (4)$$

where $S = \rho^4 - m^2 - 2m + 2\rho^2\cos 2\theta$ and $\tau_{\rho\rho}$, $\tau_{\rho\theta}$ and $\tau_{\theta\theta}$ are the stress components expressed in elliptical coordinate system (ρ, θ) [15].

The mapping between Cartesian coordinate system (x, y) and elliptical coordinate system (ρ, θ) is

† StressCheck® is a trademark of Engineering Software Research and Development, Inc., St. Louis, Missouri

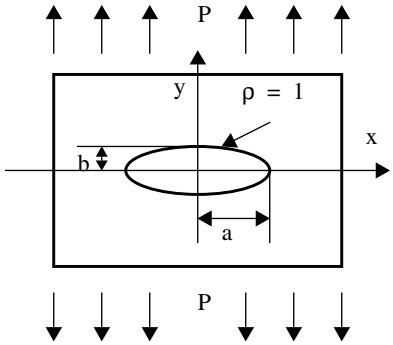

(a)

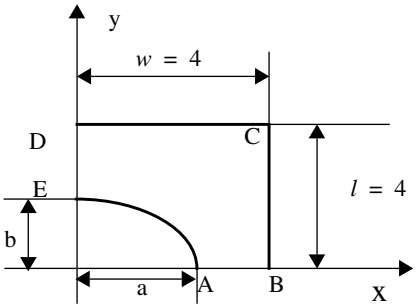

(b)

Figure 2. Elliptical hole in an infinite plane under the uniform tensile stress at infinity

$$x = R\left(\rho + \frac{m}{\rho}\right)\cos\theta \ , \quad y = R\left(\rho - \frac{m}{\rho}\right)\sin\theta \ , \ R = \frac{a+b}{2}$$

Traction (Neumann) boundary conditions are applied on edges BC and CD and symmetric Dirichlet boundary conditions are imposed on edges DE and AB.

3.2 Maximum stress and strain energy

The maximum stress σ_{max}^{exact} of this problem is concentrated at vertex A and is a function of ratio a/b only, being defined as $\sigma_{max}^{exact} = 1 + 2a/b$. The finite element stress is computed directly in this study by computing the strains from the displacement solution then applying the appropriate isotropic material stress-strain relationship. Search for the maximum computed stress σ_{max}^{fem} is conducted over not only Gauss Quadrature points but also the vertices of each element [12]. The relative error in maximum stress defined as

$$\varepsilon_{\infty} = \frac{\sigma_{max}^{fem} - \sigma_{max}^{exact}}{\sigma_{max}^{exact}} \times 100\ \% \tag{5}$$

is of great engineering interest.

The exact potential energy, Π^{exact}, of the sub-domain loaded by traction only without body force can be computed as

$$\Pi^{exact} = -\oint (T_n u_n + T_t u_t) ds \tag{6}$$

$$= -\left[\int_B^C (T_n u_n + T_t u_t) ds + \int_C^D (T_n u_n + T_t u_t) ds\right]$$

Where T_n, T_t and u_n, u_t are normal and tangential traction components and displacement components respectively [12]. The angle α measured from the positive x axis to the normal of boundaries BC and CD are $0^0, 90^0$, so Eq. (6) can be simplified as

$$\Pi^{exact} = -\left[\int_B^C (u_x \sigma_x + u_y \tau_{xy}) dy + \int_C^D (u_y \sigma_y + u_x \tau_{xy}) dx\right] \tag{7}$$

where $\sigma_x, \sigma_y, \tau_{xy}$ are stress tensor components and u_x, u_y are displacement components [4]. The exact potential energy is obtained by numerically solving Eq. (7) to an accuracy substantially greater that any of the finite element solutions. The finite element potential energy Π^{fem} is computed by evaluating the product of load vector and finite element solution over the boundary. The relative error in energy norm is defined as

$$\|\varepsilon\| = \sqrt{\left|\frac{\Pi^{exact} - \Pi^{fem}}{\Pi^{exact}}\right|} \times 100\ \% \tag{8}$$

3.3 Finite element meshes and geometric approximation shapes

A parameter $m = 0.25$ is selected to construct the first test model. An isotropic material with Young's Module of 1.0 and Poisson's ratio of 0.3 is used under the assumption of plane strain. The stress applied at the infinite boundary is 1.0. Table 1 provides the exact potential energy (to 7 digits significant figures) and the exact stress.

Table 1: Test problem

m	a	b	a/b	σ_{max}^{exact}	Π^{exact}
0.25	1.25	0.75	1.667	13/3	-7.8462131

The finite element method used for solving the problem consists of a double discretization. First, a mesh is introduced in order to discretize the geometrical domain. Then, the solution function space is approximated by a finite dimensional function space. Both geometrical and function space approximations introduce discretizations errors into the solution. In this work, we use polynomials for both discretizations where p represents the polynomial order for function space discretization and q represents the polynomial order for geometrical discretization.

The discretization error of the finite element method can be written as the sum of two contributions:

$$E^{fem} = E_p^{fem} + E_q^{fem} \tag{9}$$

where E_q^{fem} is the geometrical error and E_p^{fem} is the func-

tional error. Studies of the convergence and accuracy of the finite element method for domains where geometrical error, E_q^{fem}, is identically zero or carefully controlled to be small, thus allowing study of the functional error, E_p^{fem}, are common. We investigate the total error when the geometrical discretization error, E_q^{fem}, contribution can be significant. In this study a coarse mesh with only one edge classified on the ellipse AE (see Figure 3) is used to perform the analysis and function polynomial orders from $p = 2$ to $p = 10$ are used and geometric polynomial orders from $q = 1$ to $q = 4$ are used. (A more complete study including additional mesh configuration and geometric approximation details is in preparation for publication [4])

For the mesh edge that is used to geometrically discretize the ellipse, linear (q=1), quadratic (q=2), cubic (q=3) and quartic (q=4) geometric approximations are selected. Two different fitting methods are applied for the q>1 cases. The first is a C^0 interpolant where the interpolating points are equally spaced in the parametric space of the edge. The second enforces C^1 continuity at the vertices A and E (see [4] for specifics on the construction of those geometric approximations). Close-ups of the geometric approximations in the vicinity of vertex A are shown in Figure 4.

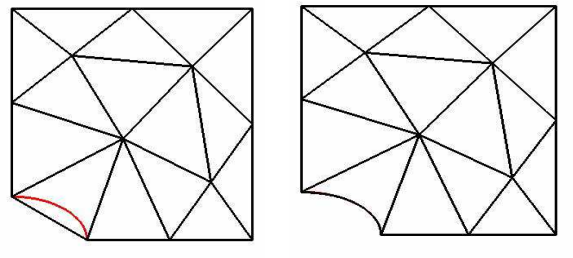

(a) Linear mesh (b) C^0 quartic mesh

Figure 3. Linear and C^0 quartic meshes

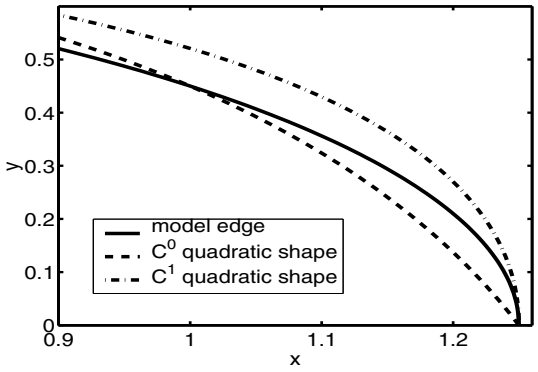

(a) C^0 and C^1 quadratic approximation shapes

Figure 4. Different geometric approximation shapes

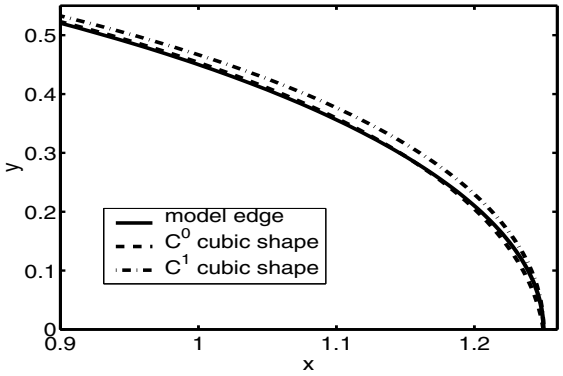

(b) C^0 and C^1 cubic approximation shapes

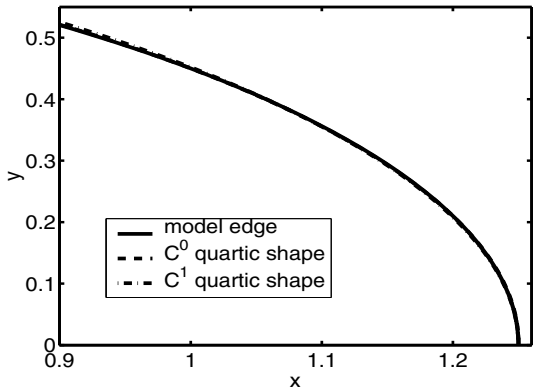

(c) C^0 and C^1 quartic approximation shapes

Figure 4. Different geometric approximation shapes

3.4 Result analysis

Convergence curves for the relative error in energy norm with respect to polynomial order p for the various geometric approximation orders q are shown in Figure 5. When the polynomial order increases past the geometric approximation order, the error in mapping begins to dominate the solution which is consistent with the basic theory [3]. The discretization error approaches a limit as p increases. This limit is essentially the E_q^{fem} because for very high p we solve the PDE nearly exactly on an approximated geometrical domain. The geometrical error E_q^{fem} is less when the geometric approximation order increases.

The performance of the different geometric approximations on the L^∞ norm of the maximum stress is a bit more complex. Figure 6a shows the relative error in maximum stress for the C^0 geometric approximations and Figure 6b shows it for the C^1 geometric approximations. For $q = 1$ (which is C^0) the computed maximum stress is underestimated at $p = 1$, but quickly increases past the exact value to overestimate the exact value by relative error of 122% at $p = 10$. Such behavior is expected since as p increases we are moving toward the solution of a problem with a sharp corner at point A where the stress theoretically goes to infinity. As q is increased for the C^0 case the sharp-

ness of the slope discontinuity at vertex A is decreased and the stress results become more accurate. However, it is interesting to note that in the case of the quadratic C^0 geometric approximation the stress is overpredicted by 45%, this is because the curved edge is not perpendicular to the symmetry plane due to the error in mapping.

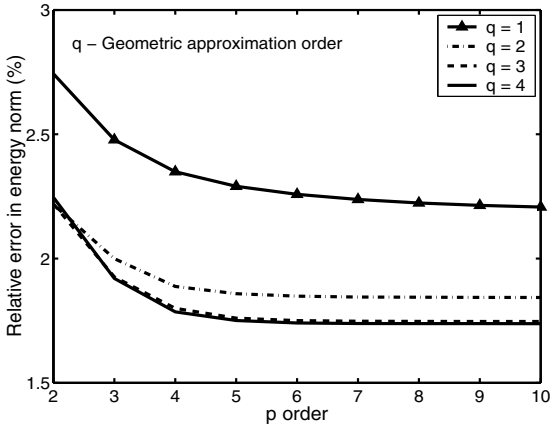

(a) Relative error in energy norm for C^0 shapes

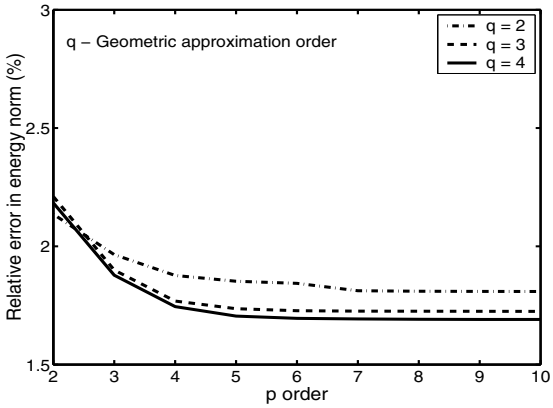

(b) Relative error in energy norm for C^1 shapes

Figure 5. Relative error in energy norm of different p, q

A comparison of the C^0 and C^1 geometric approximations cases indicates that they underestimate the exact value for low order p. In the case of the C^0 geometric approximations the stress becomes overestimated when p continues to increase. In the case of the C^1 geometric approximations the stress is always underestimated for $q = 2$ and $q = 3$ while the $q = 4$ does slightly overestimate the value for high p. Figure 7 provides a more direct comparison of the C^0 and C^1 cases for the various geometric orders.

It should be noted that the geometric approximation error for the quadratic geometric approximations, $q = 2$, at $p = 10$ are substantial with an overestimate of 45% for the C^0 case and underestimate of 16% for the C^1 case. The cubic geometric approximations, $q = 3$, yield a smaller error at $p = 10$ with an overestimate of 7.7% for

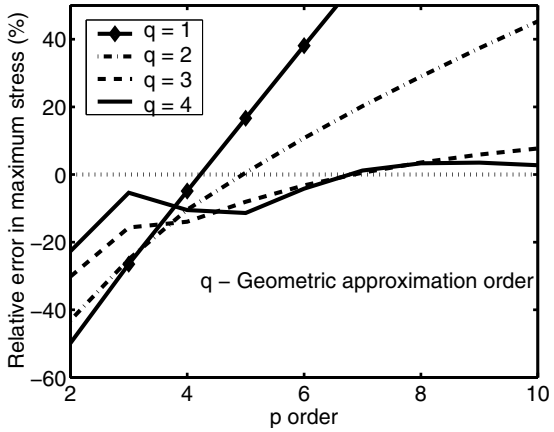

(a) C^0 interpolation shape

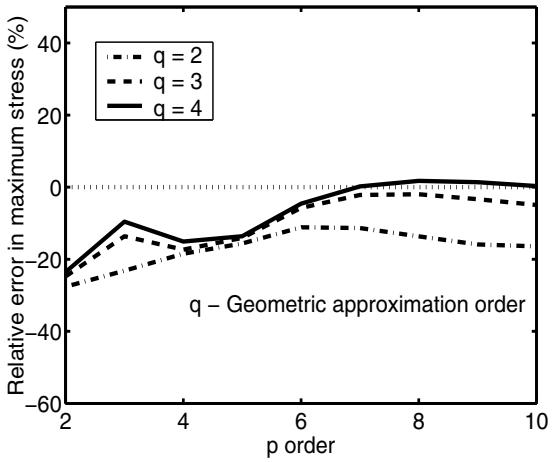

(b) C^1 continuous shape

Figure 6. The convergence curve of relative error in maximum stress for different shapes

the C^0 case and underestimate of 5.0% for the C^1 case. The quartic geometric approximations, $q = 4$, yield the smallest error at $p = 10$ with an overestimate of 2.8% for the C^0 case and 0.29% for the C^1 case. These results are consistent with those presented in reference [15] where the ellipse geometry was approximated using a blending function method.

4. CURVILINEAR MESH GENERATION

Simmetrix Inc. is developing tools to generate meshes with curved elements given an initial linear mesh. The current development efforts are aimed at the effective representation and definition of meshes consisting of mixed geometric order elements as shown in Figure 8.

4.1 Representing Mesh Shape

In the current work Bezier representations [5,6] are being used to define the mesh geometry instead of the more standard Lagrange interpolations due to the following properties of Bezier polynomials:

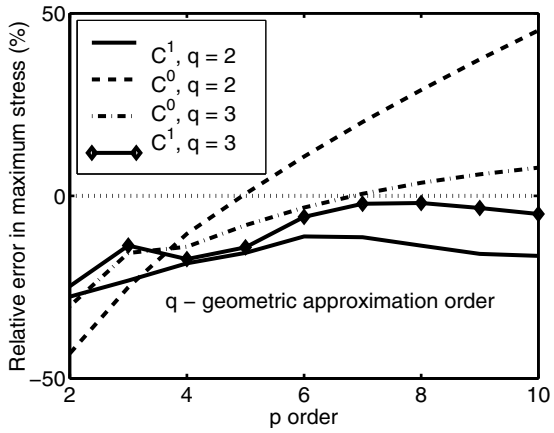

(a) Convergence curve for $q = 2, 3$

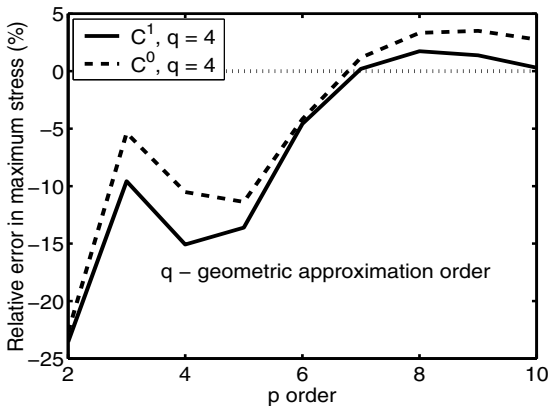

(b) Convergence curve for $q = 4$

Figure 7. Convergence curve for C^0 and C^1 shapes

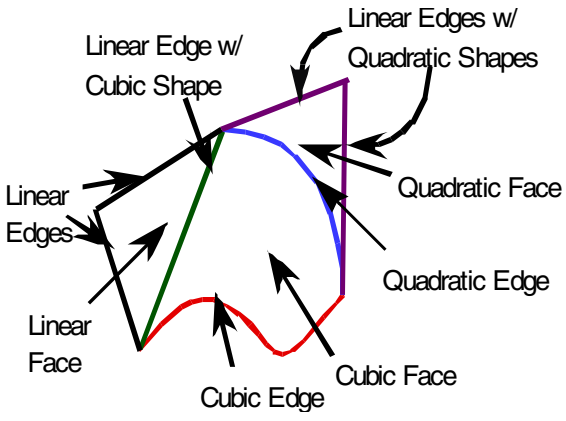

Figure 8. Example of mesh entities composed of different polynomial orders

- Convex Hull Property: A Bezier curve, surface, or volume is contained in the convex hull formed by its control points.
- As with other approximating bases, it has good shape preserving properties.
- Better qualified properties to allow more efficient intersection calculations.
- All derivatives are also Bezier functions and can be easily computed.
- Products of Bezier functions are easily computed and are a Bezier function.
- Computationally efficient algorithms for degree elevation and subdivision are available. These can be used to refine the shape's convex hull as well as adaptively refine the mesh's shape.
- Variation Diminishing Property: an infinite plane can not intersect a Bezier curve more times than it intersects control polygon.

Two major issues involved with generating curved meshes are determining if an entity's curved shape is valid, and if two or more mesh entities intersect outside of shared boundaries. In terms of the intersection issue, application of the variation diminishing property for mesh edges and the convex hull property for mesh faces has resulted in computationally efficient tests to determine if entities interfere with each other.

4.2 Determining Shape Validity

In the case of determining the validity of a mesh entity's shape, previous implementations only tested the validity of mesh regions at the integration sites that were to be used in performing the analysis. The method assumes a region is valid if the Jacobian is greater than zero at the integration sites. Though this approach is sufficient for analysis in which the element shape, order and integration rule are fixed, it suffers from the following drawbacks:

- If the analysis changes the integration rule then the integration locations will change. As a result a region that was considered valid may suddenly become invalid. The only way to use this approach would be to test each region with respect to all the possible integration sites which can be a large number of evaluations when the polynomial order of the element can be increased.
- The test itself does not provide insight on how the region can be made valid either by changing the region's topology or its geometry.
- The test only focused on mesh regions. If a mesh edge or face were invalid (due to self-intersection) then all regions using it as part of its boundaries would also be invalid. Identifying and correcting these lower dimension mesh entities would effectively reduce the number of invalid mesh regions that need to be corrected.

Instead of checking for local validity of a mesh entity's shape, Simmetrix has developed an approach based on the above Bezier properties to test for the global validity of a mesh entity. In the case of a region, the global validity check function is based on the fact that the Jacobian function can be represented as a box product of partial derivatives. In the case of a Bezier volume, the partial derivatives are also Bezier functions. Combining the 3 partials to form the Jacobian also results in a polynomial that can be represented in Bezier form. Since a Bezier polynomial is bounded by its convex hull of control points, the Bezier form of the Jacobian provides bounds on the Jacobian itself. If all the control points of the Jacobian are greater than zero then the region's Jacobian must be greater

than zero everywhere. The test works for any polynomial order. The test also provides additional information in the case of an invalid shape in terms of possible modifications that can be used to correct the shape, see Figure 9. The top image shows four mesh faces made invalid due to the curving of four mesh edges classified on the circular hole. The center image is a close up of one of the invalidities. One possible solution to this problem would be to curve each of the faces' remaining linear edges in order to resolve the invalidities. The result of these shape modifications are shown in the bottom image.

One important piece needed for curvilinear mesh generation that is missing is the aspect of mesh quality of curved meshes. Quality metrics are extremely important when choosing which mesh modification to apply in order to correct an invalid mesh shape. For example, another solution to the problem posed in Figure 9 is to relocate the faces' vertices opposite to curved edges.

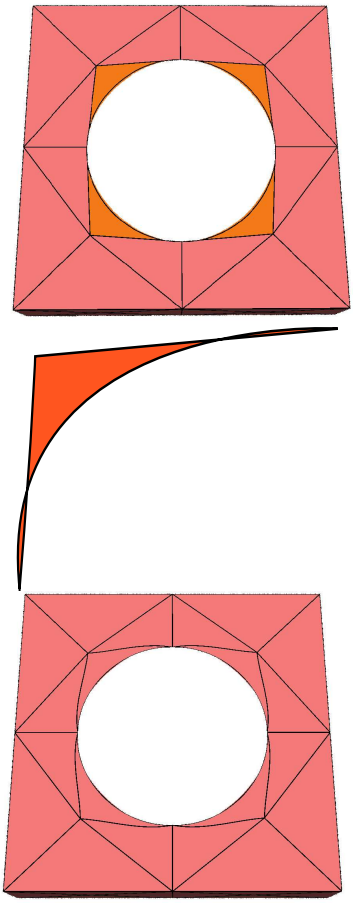

Figure 9. The effect of curving mesh edges classified on the planar face in order to correct the original highlighted invalid mesh faces

4.3 Approximating the Model's Boundary

Another important issue is how to best approximate the model boundary. As previously discussed, the approximation error between the original geometric model and the mesh can have a strong impact on the analysis. Currently interpolation methods are used to "fit" the mesh boundary to the model boundary at certain sample points on the boundary; however, using traditional methods, such as chord length interpolation [9], can cause undesirable boundary artifacts. In polynomial surfaces that are beyond quadratic. One of the major issues is to find appropriate parametric locations for the interpolation points that are not on the edges of a triangular surface. Optimization techniques that improve the quality of the surface mesh by reducing these artifacts need to be investigated. Simmetrix has implemented one such technique as shown in Figure 10..

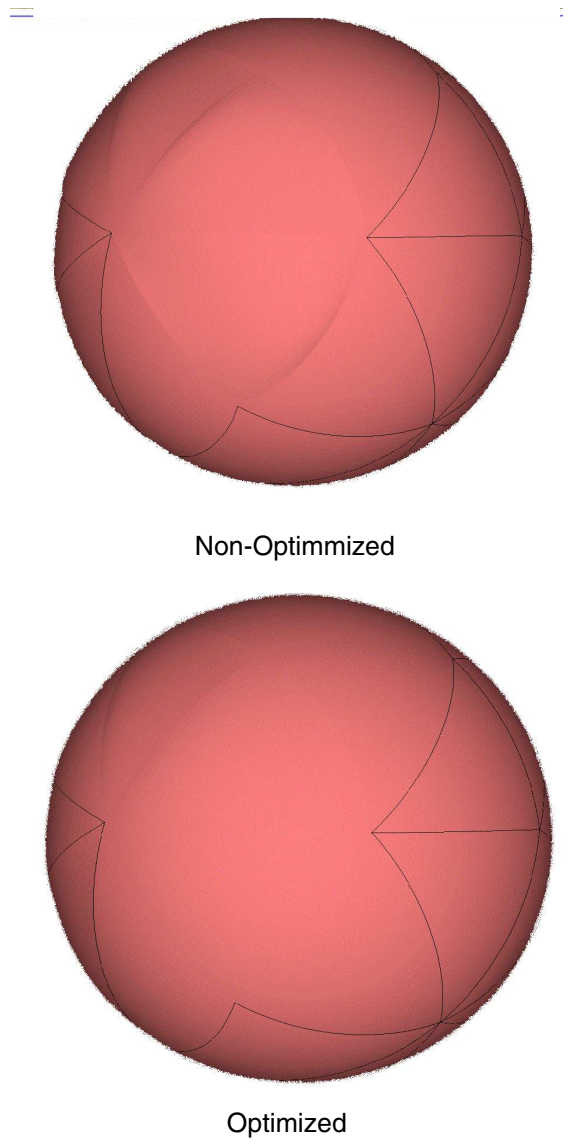

Figure 10. Comparison of non-optimized mesh faces with optimized mesh faces

Both meshes use the same interpolation points. However, the top image shows very pronounced "creases" on the sphere's surface. In the bottom image the creasing is much less pronounced.

As previously mentioned, in addition to basic interpolation

approaches, constraints such as the order of geometric continuity between mesh entities need to be taken into consideration when meshing the boundary.

4.4 Preliminary Results

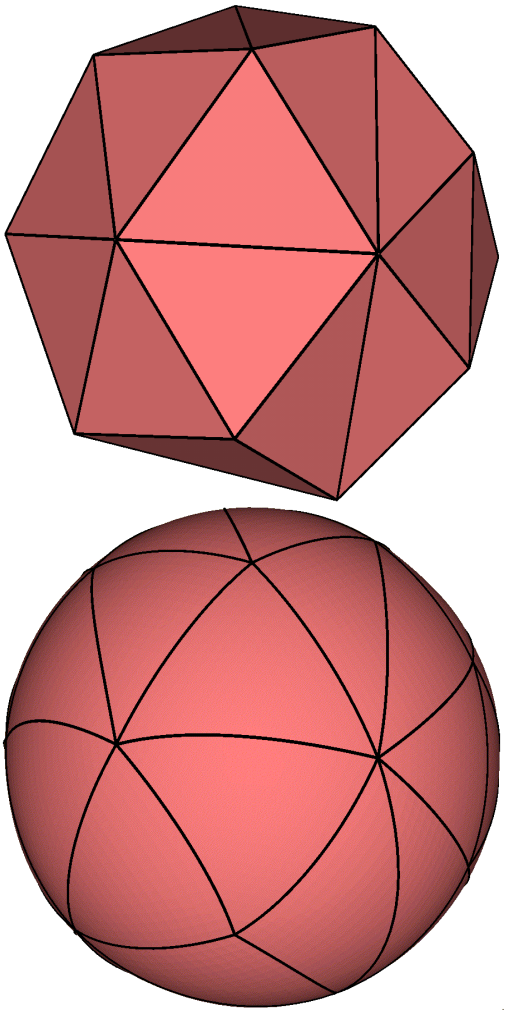

Figure 11. The result of curving a straight sided mesh classified on a sphere using a maximum polynomial degree of 3.

Figure 11 shows the result of generating a curved mesh of maximum polynomial degree q = 3 from a linear mesh. The boundary mesh entities' shapes have been optimized to reduce undesirable artifacts. Figure 12 shows a more complex example of curve mesh generation as well as the impact raising the polynomial degree on the boundary mesh. Figure 13 and Figure 14 show the application of quadratic curving on models supplied by ESRD. The initial linear meshes show the desired coarseness of the meshes.

5. CLOSING REMARK

The p-version finite element method provides an effective method to apply simulation technologies in engineering design. However, as this paper has pointed out, the applica-

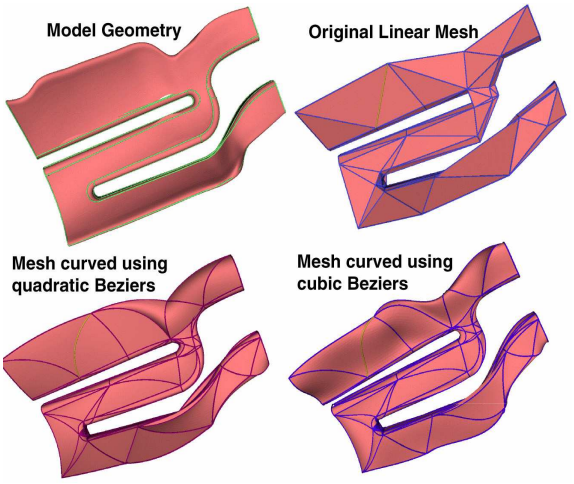

Figure 12. More complex curving example showing how the polynomial degree affects the shape of the highlighted mesh edge.

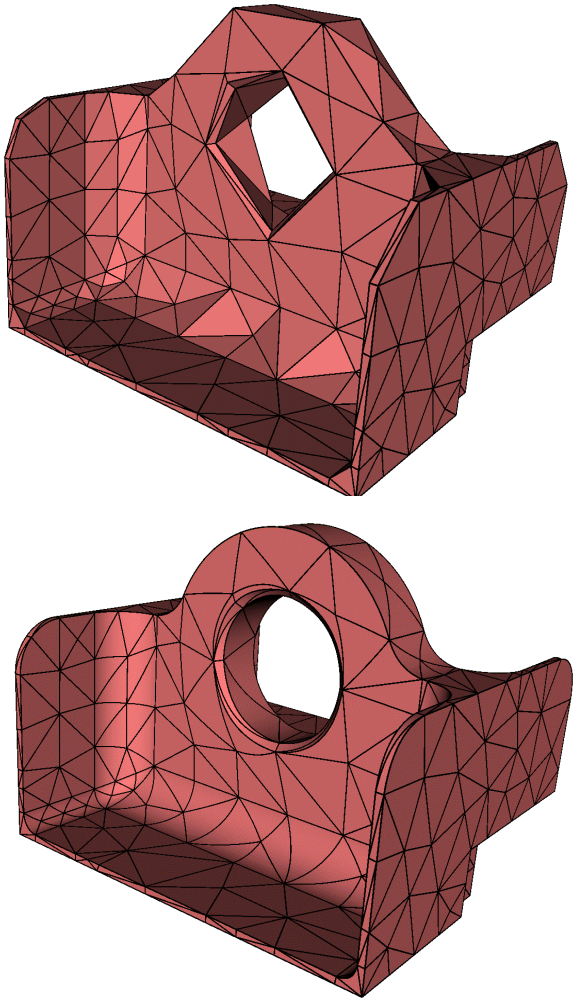

Figure 13. The application of Simmetrix's quadratic curving tool on a model supplied by ESRD.

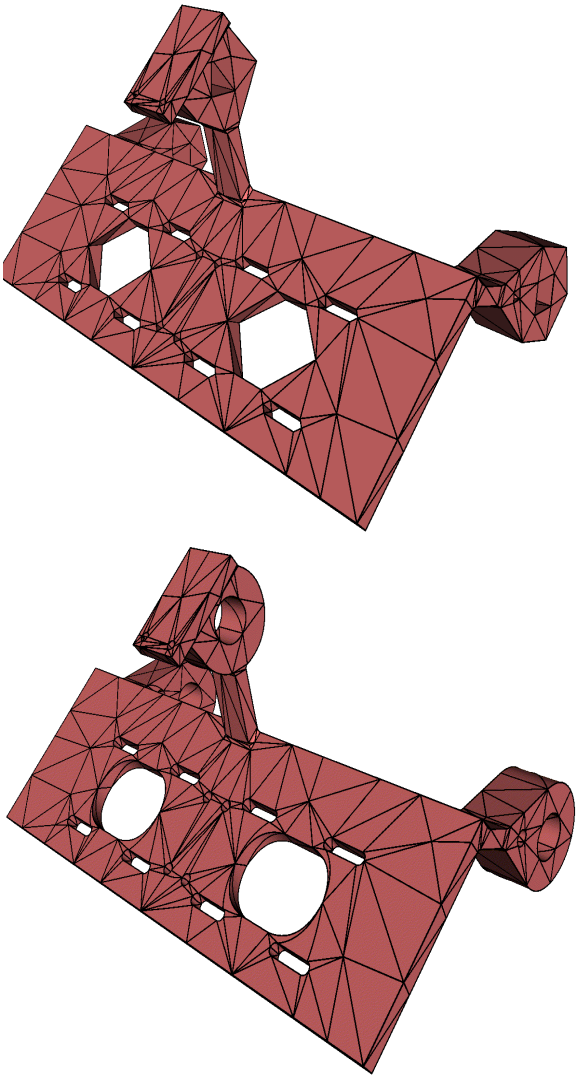

Figure 14. Another example of the quadratic curving tool on a model supplied by ESRD.

tion of these methods requires the careful construction of the meshes and control of their geometric approximation to curved domains. The brief introduction to the methods currently under development to support p-version mesh generation indicate the need to address a number of issues that do not need to be considered when low order finite elements are to be used.

6. ACKNOWLEDGEMENTS

Aspects of this work are supported by the National Science Foundation (DMI-0132742) and the Office of Naval Research (N00014-99-0725).

7. REFERENCES

[1] I. Babuska and B. Szabó, "Trends and New Problems in Finite Element Methods", *The Mathematics of Finite Elements and Applications*, J.R. Whiteman, Ed, John Wiley and Sons, Chichester, pp. 1-33 (1997)

[2] Q. Chen and I. Babuska, "Approximate Optimal Points for Polynomial Interpolation of Real Functions in an Interval and in a Triangle", *Comput. Methods Appl. Mech. Engrg.*, Vol. 128, pp. 405-417 (1995).

[3] S. Dey, M.S. Shephard and J.E. Flaherty, "Geometry-based issues associated with p-version finite element computations", *Comput., Methods. Appl. Mech. Engrg.*, Vol 150, pp. 39-55 (1997).

[4] X.J. Luo, M.S. Shephard and J.F. Remacle, "The effect of geometric approximation for curved domains in p-version finite element method", in preparation.

[5] G.E. Farin, *Curves and Surfaces for Computer Aided Geometric Design - A Practical Guide*, 3rd Edition. Boston: Academic Press, (1993).

[6] R.T. Farouki and V.T. Rajan, "Algorithms for polynomials in Bernstein", *Comput. Aid. Geom. Des*., Vol. 5, pp. 1-26 (1988).

[7] G. Királyfalvi and B. Szabó, "Quasi-Regional Mapping for the p-Version of the Finite Element Method," *Finite Elements in Analysis and Design*, Vol. 27, pp. 85-97 (1997).

[8] N.I. Muskhelishvili, *Some Basic Problems of the Mathematical Theory of Elasticity,* Groningen, P. Noordhoff, (1963).

[9] L. Piegl and W. Tiller, *The NURBS Book - 2nd Edition*, Berlin: Springer-Verlag (1997).

[10] B. Szabó, "The p- and hp-Versions of the Finite Element Method in Solid Mechanics," *Comput. Methods. Appl. Mech. Engrg.*, Vol. 80, pp. 185-195 (1990).

[11] B. Szabó, "On Reliability in Finite Element Computations", *Comp. & Structures*, Vol. 39, pp. 729-734 (1991).

[12] B. Szabó and I. Babuska, *Finite Element Analysis*, John Wiley & Sons New York, (1991).

[13] B. Szabó and R. Actis, "Finite Element Analysis in Professional Practice," *Comput. Methods. Appl. Mech. Engrg.*, Vol. 133, pp. 209-228 (1996).

[14] B. Szabó, "Quality Assurance in the Numerical Simulation of Mechanical Systems," C*omputational Mechanics for the 21st Century*, B.H.W. Topping, Ed., Saxe-Coburg Pub., Edinburgh pp.51-69, (2000).

[15] Z. Yosibash and B. Szabó, "Convergence of Stress Maxima in Finite elent Computations", *Comm. Numer. Methods Engrg*. Vol. 10: pp. 683-697, (1994).

[16] I. Babuska and M. Suri, "The p and h-p versions of the finite element method, basic priciples and properties", SIAM *J. Numer. Anal*., Vol. 36(4) pp. 578-631 (1994).

[17] P. Carnevall and R.B. Morris, Y. Tsuji and G. Taylor, "New basis functions and computational procedures of p-version finite element analysis, *Int. J. Numer. Methods. Engrg*, Vol. 36 pp. 3759-3779 (1993).

[18] C.G. Kim and M. Suri, "On the p-version of the finite element method in the presence of numerical integration", *Numer. Methods. Partial Differential Equations*, Vol. 9 pp. 593-629 (1993).